

RESEARCH

Open Access



# Development of two species of the *Trypanosoma theileri* complex in tabanids

Alexei Yu. Kostygov<sup>1,2\*</sup> , Alexander O. Frolov<sup>1</sup>, Marina N. Malysheva<sup>1</sup>, Anna I. Ganyukova<sup>1</sup>, Daria Drachko<sup>1</sup>, Vyacheslav Yurchenko<sup>2,3</sup> and Vera V. Agasoï<sup>1,4</sup>

## Abstract

**Background:** *Trypanosoma theileri* species complex includes parasites of Bovidae (cattle, sheep, goat, etc.) and Cervidae (deer) transmitted mainly by Tabanidae (horse flies and deerflies) and keds (Hippoboscidae). While morphological discrimination of species is challenging, two big clades, TthI and TthII, each containing parasites isolated from bovids and cervids, have been identified phylogenetically. To date, the development in the vector has been studied in detail only for the ked-transmitted sheep parasite *T. melophagium* (TthII), while the fate of trypanosomes in tabanids was described only briefly by light microscopy.

**Methods:** We collected infected tabanids of various species and identified trypanosomes by molecular phylogenetic analysis. The morphology and development of trypanosomes was studied using the combination of statistical analyses as well as light and electron microscopy.

**Results:** Two trypanosome species belonging to both TthI and TthII clades of the *T. theileri* complex were identified. The phylogenetic position of these two trypanosomes suggests that they parasitize deer. Both species were indiscernible by morphology in the vector and showed the same development in its intestine. In contrast to the previously described development of *T. melophagium*, both trypanosomes of tabanids only transiently infected midgut and settled mainly in the ileum, while pylorus and rectum were neglected. Meanwhile, the flagellates developing in the tabanid ileum (pyriform epimastigotes and metacyclic trypomastigotes) showed similarities to the corresponding stages in *T. melophagium* by morphology, mode of attachment to the host cuticle and formation of the fibrillar matrix surrounding the mass of developing parasites. In addition, for the first time to our knowledge we documented extraintestinal stages in these trypanosomes, located in the space between the epithelium and circular muscles.

**Conclusions:** The development of different species of flagellates of the *T. theileri* complex in their insect vectors shows many similarities, which can be explained not only by their common origin, but also the same transmission mode, i.e. contamination of the oral mucosa with the gut content released after squashing the insect either by tongue or teeth. The observed differences (concerning primarily the distribution of developmental stages in the intestine) are associated rather with the identity of vectors than the phylogenetic position of parasites.

**Keywords:** Trypanosomes, Life cycle, Vector, Horseflies, Deerflies

## Background

*Trypanosoma theileri* is one of the first trypanosome species described in mammals [1]. It was originally characterized in cattle from Transvaal (now Republic of South Africa) and later documented in various bovines throughout the world, often under different names, which were subsequently synonymized with *T. theileri*

\*Correspondence: kostygov@gmail.com

<sup>1</sup> Zoological Institute of the Russian Academy of Sciences, St. Petersburg 190121, Russia

Full list of author information is available at the end of the article



© The Author(s) 2022. **Open Access** This article is licensed under a Creative Commons Attribution 4.0 International License, which permits use, sharing, adaptation, distribution and reproduction in any medium or format, as long as you give appropriate credit to the original author(s) and the source, provide a link to the Creative Commons licence, and indicate if changes were made. The images or other third party material in this article are included in the article's Creative Commons licence, unless indicated otherwise in a credit line to the material. If material is not included in the article's Creative Commons licence and your intended use is not permitted by statutory regulation or exceeds the permitted use, you will need to obtain permission directly from the copyright holder. To view a copy of this licence, visit <http://creativecommons.org/licenses/by/4.0/>. The Creative Commons Public Domain Dedication waiver (<http://creativecommons.org/publicdomain/zero/1.0/>) applies to the data made available in this article, unless otherwise stated in a credit line to the data.

(reviewed in [2]). Similar trypanosomes have also been described from other ruminants: *T. melophagium* from sheep, *T. theodori* from goat, *T. ingens* from antelopes and cattle, as well as *T. mazamarum*, *T. cervi*, *T. stefanskii*, and *T. trinaperronei* from various cervids [2–6]. It is not clear how reliable the discrimination of all these species was, given that most of them differed by size characters and trypanosomes are known to manifest pleomorphism (significant variation in size and shape during development) [2]. However, cross-infection experiments demonstrated that deer trypanosomes are not infective to cattle, and, vice versa, the flagellates from cows cannot settle in cervids [4, 7].

The large size of these trypanosomes (40–100  $\mu\text{m}$ ) was considered a distinctive feature and justified their separation (together with similar parasites from other hosts, e.g. monkeys and bats) into the subgenus *Megatrypanum* with *T. theileri* as the type species [8]. This trait was indeed important to discriminate these flagellates from other trypanosomes of livestock, such as *T. vivax*, *T. congolense*, and *T. brucei* ssp. causing severe diseases collectively named African animal trypanosomiasis. In contrast, species of the subgenus *Megatrypanum* are typically considered non-pathogenic [2]. Nevertheless, there are multiple reports that *T. theileri* can be an opportunistic pathogen acting in synergy with viruses or piroplasmids, or even be able to cause mild to severe symptoms alone, sometimes leading to death in fetuses and neonate calves [9–18].

Phylogenetic analyses performed using several molecular markers on a wide range of *Megatrypanum* isolates from various ruminants and blood-sucking dipterans demonstrated that although this group is monophyletic, it consists of several lineages united into two big clades, TthI and TthII, each containing parasites isolated from bovids and cervids [6, 19–24]. Thus, the whole group is considered *T. theileri* species complex [25], within which only *T. melophagium* and recently described *T. trinaperronei* can be identified with certainty. For other species of the complex including *T. theileri*, it is currently impossible until a scrupulous taxonomic revision is performed.

Most trypanosomes of the complex are transmitted by Tabanidae (horseflies and deerflies), while keds (Hippoboscidae) serve as vectors for *T. melophagium*, *T. trinaperronei*, and *T. theodori* [2, 6]. *Trypanosoma theileri*-like trypanosomes were also documented in various mosquitoes, a sandfly, and a tsetse fly [26–28]. In addition, *T. theileri* has been repeatedly reported in ticks [29–32]. However, the only study assessing the phylogenetic position of a trypanosome from a cattle-associated tick demonstrated that it is phylogenetically distant from *Megatrypanum* and is closely related to the poorly studied *T. pestanaei* clade [33]. Experiments with transmission

of *T. melophagium*, as well as trypanosomes of cattle and deer, have demonstrated that infection of mammalian hosts is achieved only when vector gut content is applied to the oral mucosa (which does not need to be damaged), while routes known in other trypanosomes (through a bite or via abraded skin) are ineffective [7, 34, 35].

Studies of the development of *Megatrypanum* from ruminants in vectors started at the beginning of the twentieth century, even before it became clear that the flagellates in the guts of keds and tabanids are trypanosomes [36–38]. Later, there was an attempt to investigate the development of *T. theileri* in tabanids with light microscopy using parasite-free insects fed on an infected cow [39]. Thus, the sequential colonization of different gut sections and transformation of cell types have been observed, but details of the host-parasite relationships and the ultrastructure of trypanosomes have not been described. A similar study has been performed for *T. theodori* vectored by the goat ked *Lipoptena capreoli* [2]. More attention has been paid to *T. melophagium*, whose development in the sheep ked has been studied in detail using light as well as transmission and scanning electron microscopy. This illuminated the distribution of parasites across the gut, continuity of the developmental stages, modes of cell attachment, etc. [40–42]. It is furthermore surprising that the main vectors of *T. theileri*-like trypanosomes remained virtually neglected.

In this work, we described the development of two species belonging to the TthI and TthII clades of the *T. theileri* complex in tabanids using light and electron microscopy and demonstrated that it is similar in both cases, although distinct from that of *T. melophagium*. In addition, for the first time, we documented presence of extraintestinal stages of these parasites in insect vectors.

## Materials and methods

### Hosts collection, dissection, and isolation of trypanosome-containing gut sections

Tabanids attacking the authors of this work were manually collected into individual vials with water-containing tubes in 2018, 2020, and 2021 in four locations in the Northwestern Federal District of Russia (Table 1). Within 24 h after their capture, the insects were killed with chloroform and dissected in normal saline. The entire digestive tube (Fig. 1) was isolated, carefully placed on a slide, covered with a cover glass, and inspected under light microscope. After detection of infection, the corresponding parts of the intestine were used for smear preparation, DNA isolation, or electron microscopy.

### DNA isolation, PCR and sequencing

Infected intestine fragments, preserved in the solution containing 1% SDS and 50 mM EDTA after dissection,

**Table 1** Isolates of trypanosomes studied in this work

Isolate	Species	Host (vector)	Locality	Year
194Tab	Ttha	<i>Hybomitra solstitialis</i> <sup>b</sup>	Karelia, Lakhdenpokhya town (61°31'N, 30°12'E)	2018
KrSL1 <sup>a</sup>	Tthβ	<i>Hybomitra tarandina</i>		
KrSL4 <sup>a</sup>	Ttha	<i>Hybomitra muehlfeldi</i>		
KrSL7 <sup>a</sup>	Ttha	<i>Chrysops divaricatus</i>		
513SL	Tthβ	<i>Hybomitra muehlfeldi</i>	Leningrad Oblast, Bol'shoye Rakovoye Lake (60°37'N, 29°22'E)	2020
519SL	Tthβ			
D1011	Tthβ	<i>Hybomitra bimaculata</i>	Leningrad Oblast, Toksovskoye village (60°09'N, 30°35'E)	2021
D1012	Ttha	<i>Hybomitra muehlfeldi</i>		
D1013	Ttha	<i>Chrysops viduatus</i>		
D1016	Ttha	<i>Hybomitra solstitialis</i> <sup>b</sup>		
D1017	Ttha	<i>Hybomitra bimaculata</i>		
F1187	Tthβ	<i>Hybomitra nitidifrons conformis</i>	Novgorod Oblast, Oksochi village (58°39'N, 32°47'E)	2021
F1206	Ttha			

<sup>a</sup> Isolated in a previous study [43]

<sup>b</sup> *H. solstitialis* (Meigen, 1820) = *H. ciureai* (Séguy, 1937)

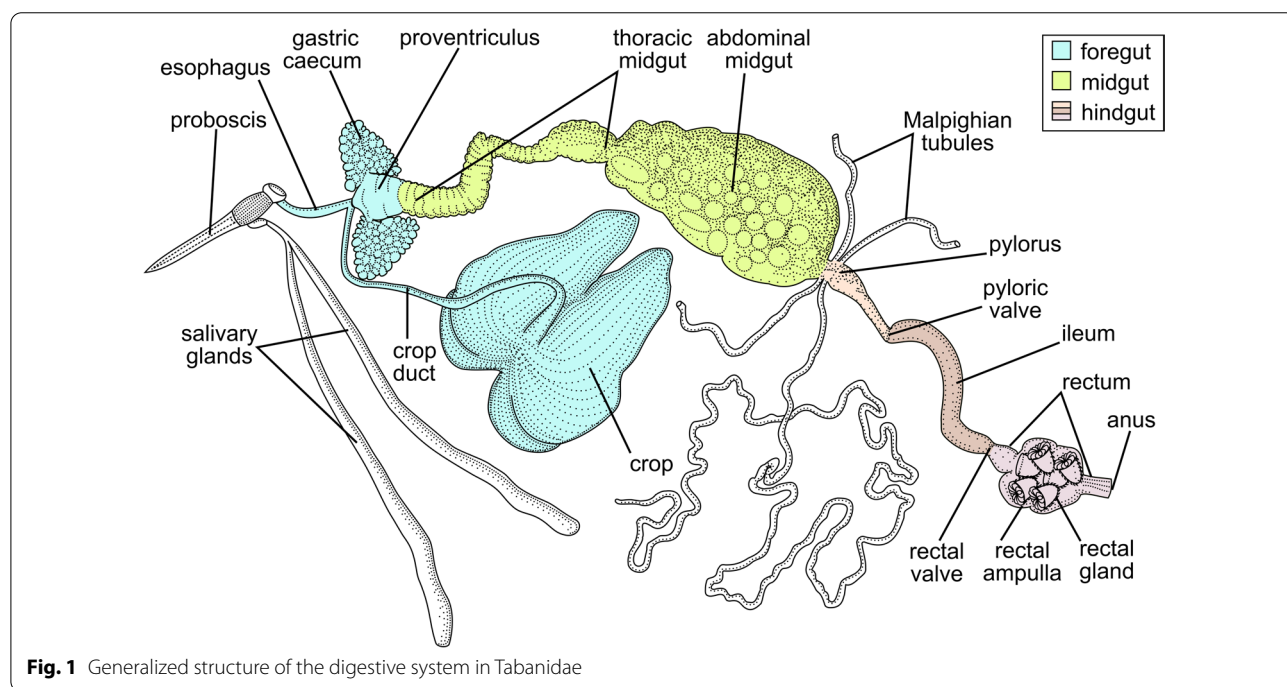


**Fig. 1** Generalized structure of the digestive system in Tabanidae

served to identify trypanosomes. Total DNA was isolated from these samples with the DNeasy Blood & Tissue Kit (Qiagen, Hilden, Germany) following the manufacturer's protocol. This DNA was used to specifically amplify either the nearly full-length trypanosomatid 18S rRNA gene with the primers S762 and S763 [44] or its 836-bp fragment (encompassing variable regions V8, V3, V4 and V9) with the primer pair 1127F (5'-aggcattcttcaag gataccttcc-3') and 1958R (5'-tgatgagctgagcctacgaga-3') [45]. A ~900-bp fragment of the glycosomal

glyceraldehyde-3-phosphate dehydrogenase (gGAPDH) gene was amplified using the primers G3 and G4a [46]. PCR fragments were sequenced using either amplification primers or, in the case of the full-length 18S rRNA gene, a set of internal primers as described before [47]. Samples showing mixed signal were excluded from subsequent analyses. The sequences were deposited in GenBank under accession numbers OL855997–OL856006 (18S rRNA gene) and OL860973–OL860974 (gGAPDH gene).

### Phylogenetic analyses

The nucleotide sequences obtained in this study along with related ones retrieved from GenBank were aligned by MAFFT v. 7.475 [48] using the E-INS-i and L-INS-i algorithms for the 18S rRNA and gGAPDH genes, respectively. The 18S rRNA alignment was deduplicated to preserve the longest available sequence for each haplotype, while keeping information about all sequences belonging to these haplotypes. A maximum likelihood tree was inferred in IQ-TREE v. 2.1.3 [49] under the K2P+I substitution model selected by the built-in ModelFinder module [50]. Edge support was estimated using the ultrafast bootstrap method with 1000 replicates. The phylogeny inference using the gGAPDH gene was performed by the maximum likelihood method in IQ-TREE and the Bayesian approach in MrBayes v. 3.2.7 [51] under the partitioned model (F81+F+I, JC+I and TIM2+F+G4 selected by ModelFinder for the first, second and third codon positions, respectively). Branch lengths were unlinked among the three character sets. Edge support in IQ-TREE was assessed with 1000 standard bootstrap replicates. The analysis in MrBayes was run for 10 million generations with every 100th sampled and other parameters set by default.

### Microscopy and morphometry

The ethanol-fixed smears prepared during tabanid dissection were stained with Giemsa, examined under light microscope, photographed and measured as described earlier [52]. Observed cells were classified into three main morphotypes, for which six standard morphometric features were evaluated: cell length (not including the free flagellum) and width, nucleus length, distances between the anterior end and the nucleus or kinetoplast, and free flagellum length. The results of these measurements are presented in Additional file 1: Table S1. The morphometric characters (except for the length of free flagellum that could not be reliably measured in all cells) were used for comparison of morphotypes between trypanosome species and individual isolates within a particular species by principal component analysis (PCA) in PAST 4.08 software using default settings [53]. The results were visualized as two-dimensional plots with the raw data projected onto axes representing eigenvectors extracted from calculated correlation matrices.

Sample preparation procedures for transmission electron microscopy (TEM) have been described earlier [54]. For scanning electron microscopy (SEM), glutaraldehyde-fixed fragments of tabanid guts were air dried on coverslips, which were subsequently attached to specimen stubs, coated with gold, and examined with Tescan MIRA3 LMU electron microscope at 5 kV (Tescan, Brno,

Czech Republic). These analyses were performed for the isolates 194Tab, 513SL, 519SL (TEM) and D1011-D1013, D1016 and D1017 (SEM).

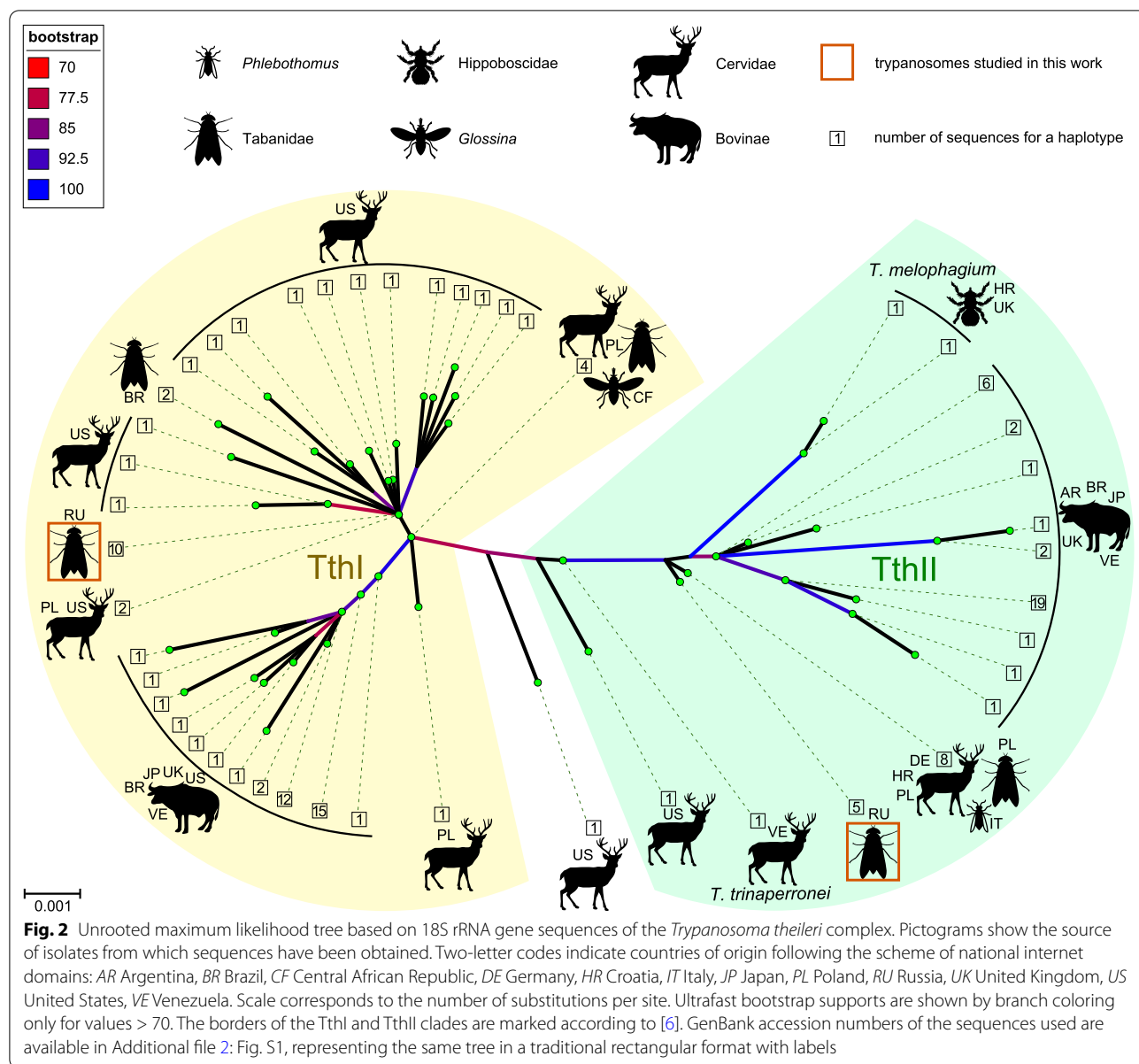
To study the distribution of trypanosomes in the hind-gut in detail, the 194Tab sample processed for (TEM) was also used to prepare serial semithin (700 nm) sections. The latter were placed on glass slides in a drop of water, then attached by drying on a warm stage at 60 °C and stained there with Richardson stain [55] for 30–60 s.

## Results

### Molecular phylogenetic analyses

The 18S rRNA gene sequences of trypanosomes from the infected gut specimens represented only two variants (haplotypes), which we have observed in a previous study [43]. These two variants were unambiguously associated with the *Trypanosoma theileri* complex, and we provisionally named them Tth $\alpha$  and Tth $\beta$ . The difference between the haplotypes consisted of eight substitutions and one 2-nt indel, considering the whole length of the 18S rRNA gene corresponds to < 0.5% difference. The phylogenetic analysis demonstrated that Tth $\alpha$  and Tth $\beta$  belong to two different clades of the *T. theileri* complex—TthI and TthII, respectively (Fig. 2, Additional file 2: Fig. S1). Within the TthI lineage, the Tth $\alpha$  species showed affinity to the cluster composed of sequences from cervids and tabanids, although the support of this cluster is low. Moreover, almost identical (differing in just a single 1-nt indel) sequences were obtained from a white-tailed deer in the USA and a tabanid in Poland. These facts suggest that Tth $\alpha$  is a deer trypanosome. As for Tth $\beta$ , its position on the 18S rRNA gene-based tree does not allow assessing the affinity of this trypanosome, although the most similar sequences were obtained from European cervids, tabanids and a sandfly.

Although the 18S rRNA gene has the advantage of a large database of sequences, it typically does not provide sufficient resolution when dealing with related species. Therefore, we applied another marker, the gGAPDH gene, which better resolves relationships between *Trypanosoma* spp. [46, 56, 57]. Indeed, the inferred tree helps to position the two trypanosomes under study with high statistical support (Fig. 3). Tth $\alpha$  again clusters with cervid trypanosomes, more specifically with those from Japanese sika deer (these isolates are not present on the 18S rRNA gene-based tree). The close relationship of Tth $\beta$  with the abovementioned group of European isolates [represented here by the isolate D30 (from a fallow deer), whose sequences are available for both genes] becomes unambiguous. Of note, the recently described *T. trinaperronei* from white-tailed deer is the next closest relative.



### Light microscopy

In all infected tabanids, trypanosomes were always present in the ileum, while in the midgut and rectum no or a few flagellates could be observed. Localization of trypanosomes in the hindgut was studied in detail for isolate 194Tab using a series of semithin sections (Fig. 4).

At most of the length of the ileum, the majority of trypanosomes are attached to the intestinal wall, completely covering its inner surface in 2–3 layers (Fig. 4a, b). However, they do not settle near the border with the rectal valve, where the ileum forms 8–10 large diverticula containing symbiotic bacteria. The latter are localized either on the cuticular lining of the epithelium or in the

diverticular lumina (Fig. 4c, d). The rectal valve and the rectal ampulla, which contains six large glands, are also free of trypanosomes (Fig. 4e, f).

The micropopulation of trypanosomes in the ileum is heteromorphic and consists of three main morphotypes (proportions increase from first to last (Table 2): free elongated epimastigotes (Fig. 5a–c), attached pyriform epimastigotes (Fig. 5d–g) and attached metacyclic trypomastigotes (Fig. 5h–k). Only epimastigotes of both types are able to proliferate (Fig. 5c, f, g). In elongated epimastigotes, the kinetoplast is localized near the anterior margin of the nucleus, which is situated in the anterior third of the cell (Fig. 5a–c). In pyriform

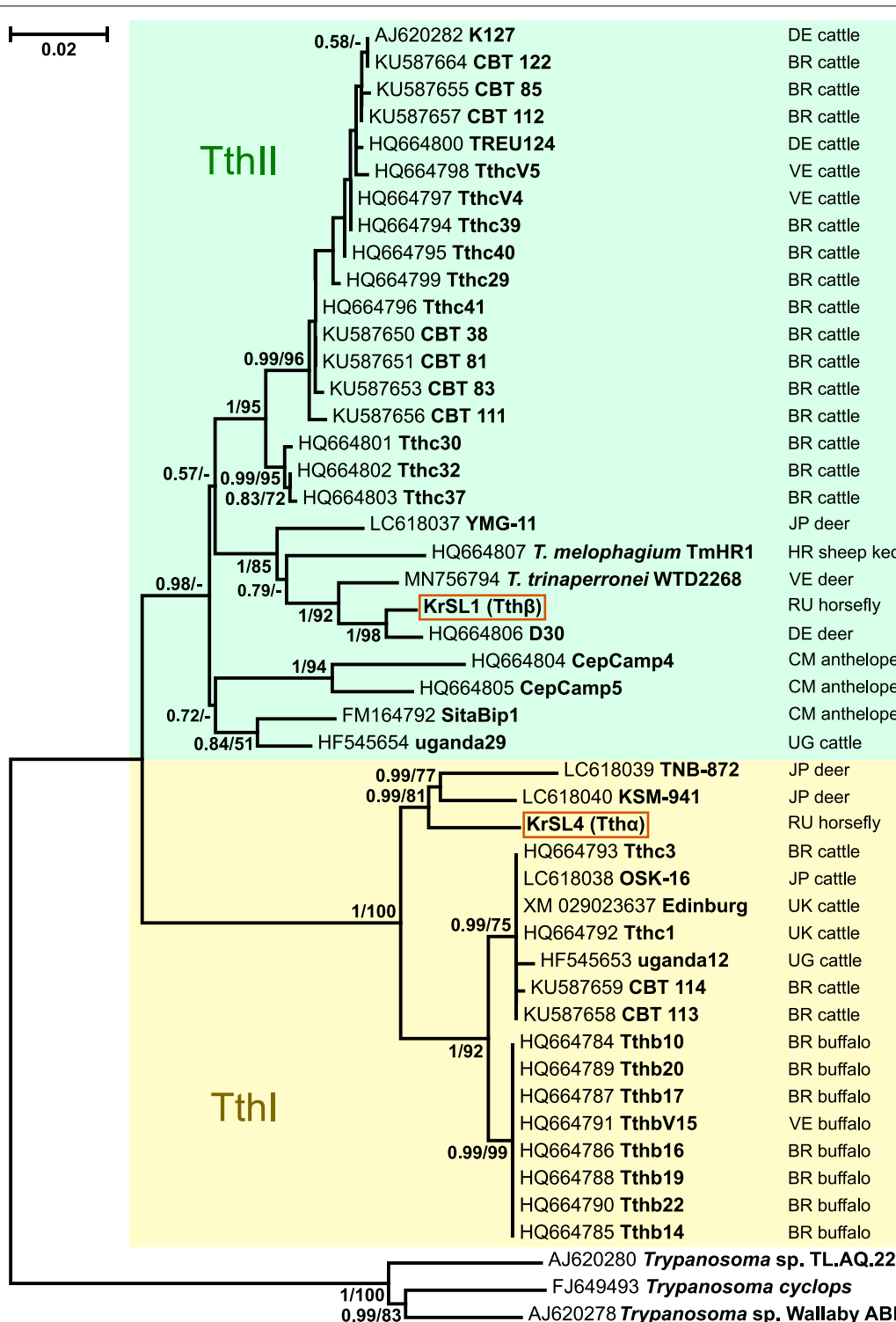


**Fig. 3** Maximum likelihood phylogenetic tree of *Trypanosoma (Megatrypanum)* spp. based on gGAPDH gene sequences. Bayesian posterior probabilities and bootstraps are shown at branches for values > 0.5 and 50, respectively. Two-letter codes indicate countries of origin following the scheme of national internet domains (BR Brazil, CM Cameroon, DE Germany, JP Japan, RU Russia, UG Uganda, UK United Kingdom, US United States, VE Venezuela). Scale corresponds to the number of substitutions per site. The borders of the TthI and TthII clades are marked according to [6]. Three sequences of trypanosomes not belonging to the *T. theileri* complex are used as outgroups (not highlighted)

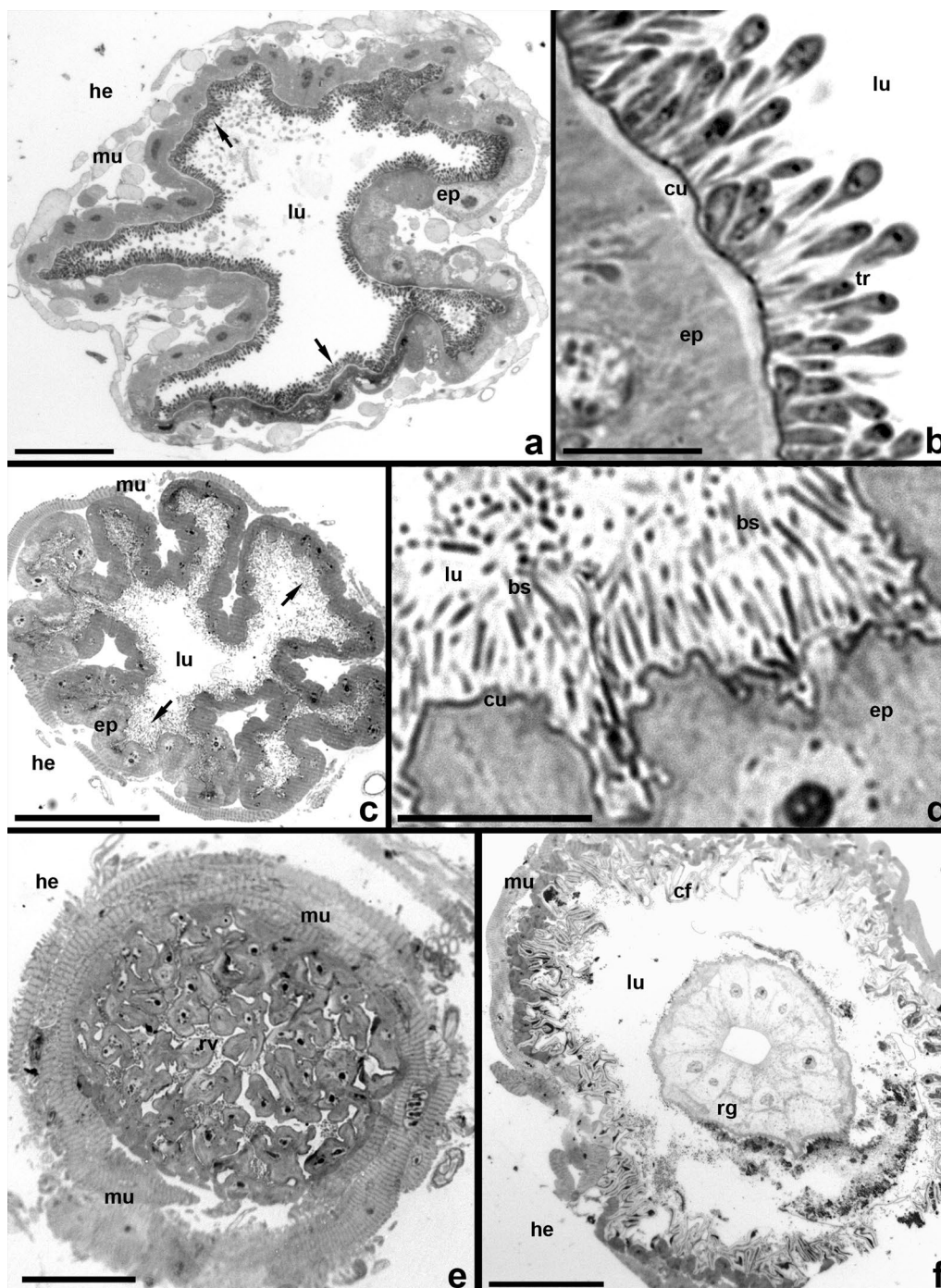


**Fig. 4** Semithin cross sections of the hindgut (isolate 194Tab). Richardson stain. **a, b** Trypanosomes on the ileum cuticle. **c, d** Posterior portion of ileum, containing only symbiotic bacteria. **e** Rectal valve. **f** Rectal ampulla with one of the six rectal glands. *bs* bacterial symbionts, *cf* cuticle folds, *cu* cuticle, *ep* intestinal epithelium, *he* hemocoel, *lu* intestinal lumen, *mu* muscles of the intestine, *rg* rectal gland, *tr* trypanosome cells. Arrows in **a** and **c** show trypanosomes and bacteria, respectively. Scale: **a** 50  $\mu$ m; **b, d** 10  $\mu$ m; **c, e** 40  $\mu$ m; **f** 100  $\mu$ m

epimastigotes, the nucleus and kinetoplast are shifted to the center of the cell but preserve their mutual arrangement (Fig. 5d, e). The products of their division

can preserve the same features (Fig. 5f) or become more similar to metacyclics, with the nucleus displaced backward and the kinetoplast migrating to its posterior

**Table 2** Proportions of cell morphotypes in the ileum

Isolates	Ttha				Tthβ	
	KrSL7	F1206	D1017	194Tab	KrSL1	513SL
Elongated epimastigotes	1.46%	2.80%	3.15%	0.56%	0.14%	0.65%
Pyriiform epimastigotes	13.99%	16.78%	5.14%	8.09%	4.12%	7.67%
Metacyclics	84.55%	80.42%	91.71%	91.35%	95.74%	91.68%
N	686	143	603	686	2934	1082

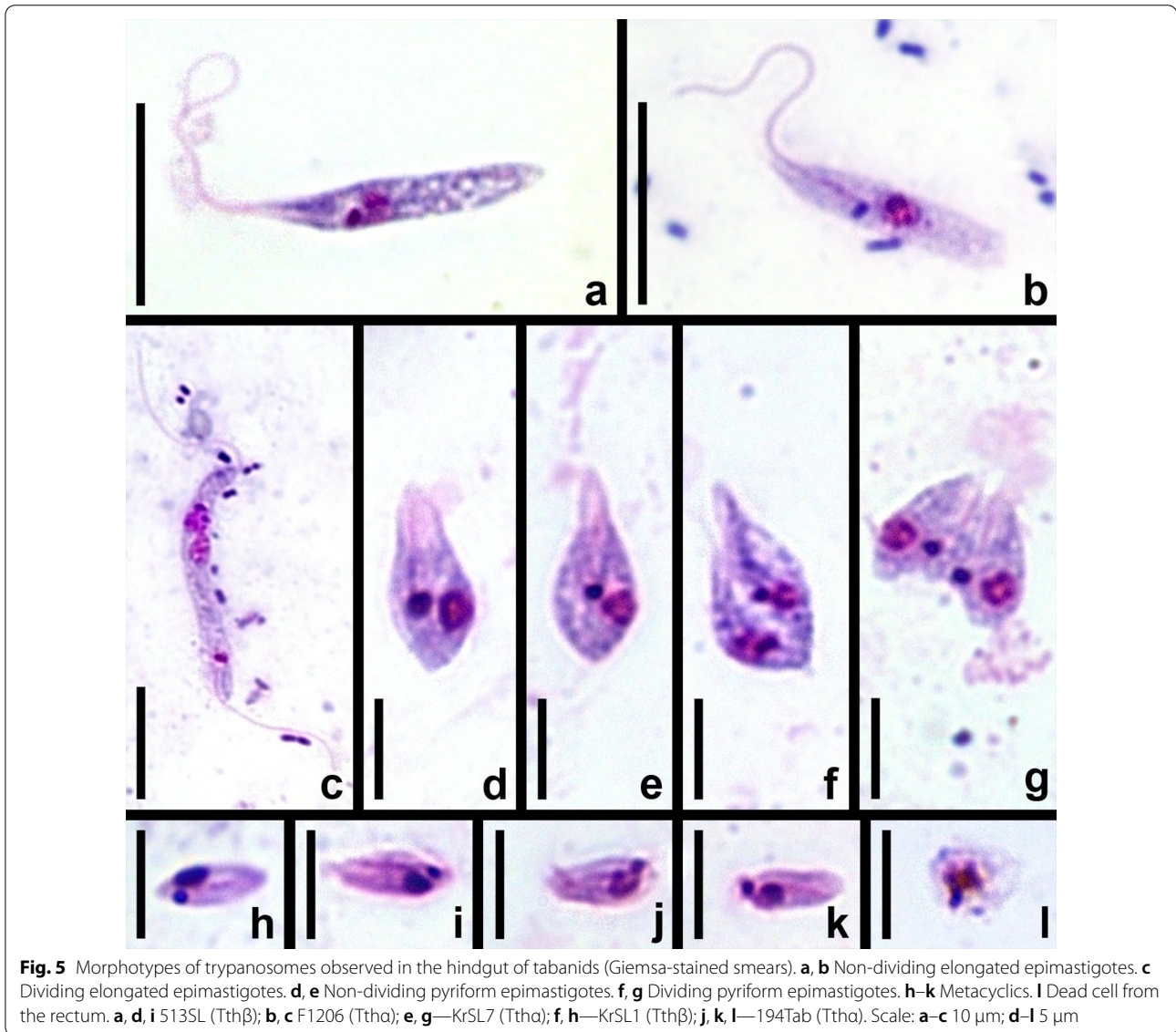


**Fig. 5** Morphotypes of trypanosomes observed in the hindgut of tabanids (Giemsa-stained smears). **a, b** Non-dividing elongated epimastigotes. **c** Dividing elongated epimastigotes. **d, e** Non-dividing pyriform epimastigotes. **f, g** Dividing pyriform epimastigotes. **h–k** Metacyclics. **l** Dead cell from the rectum. **a, d, i** 513SL (Tthβ); **b, c** F1206 (Ttha); **e, g**—KrSL7 (Ttha); **f, h**—KrSL1 (Tthβ); **j, k, l**—194Tab (Ttha). Scale: **a–c** 10 μm; **d–l** 5 μm

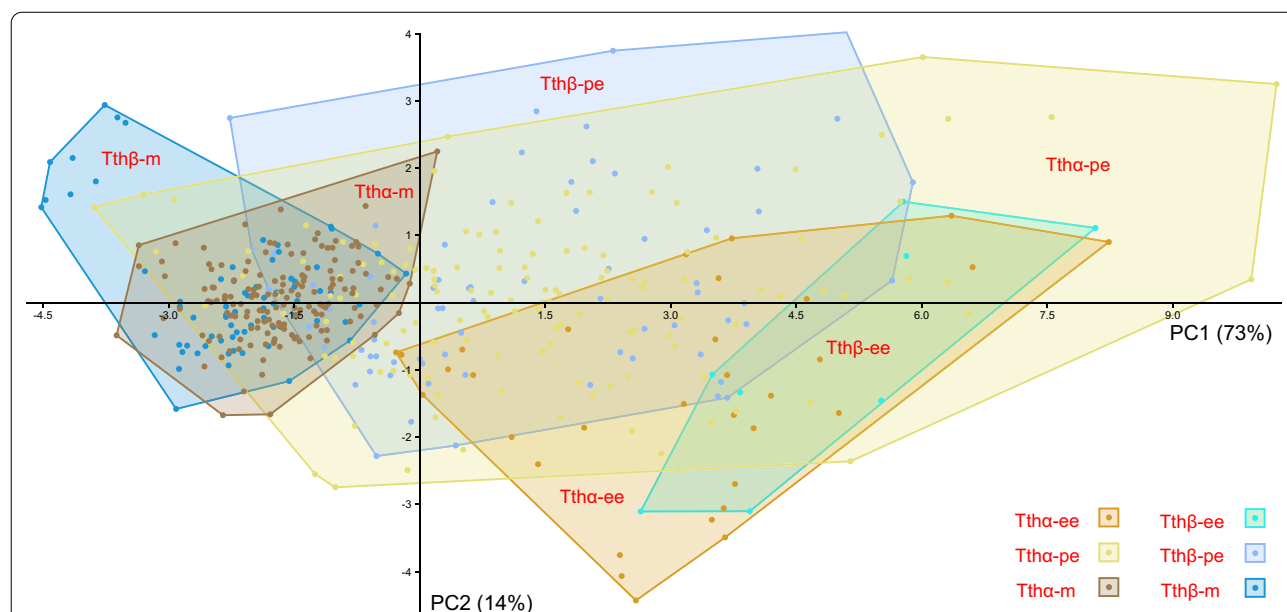
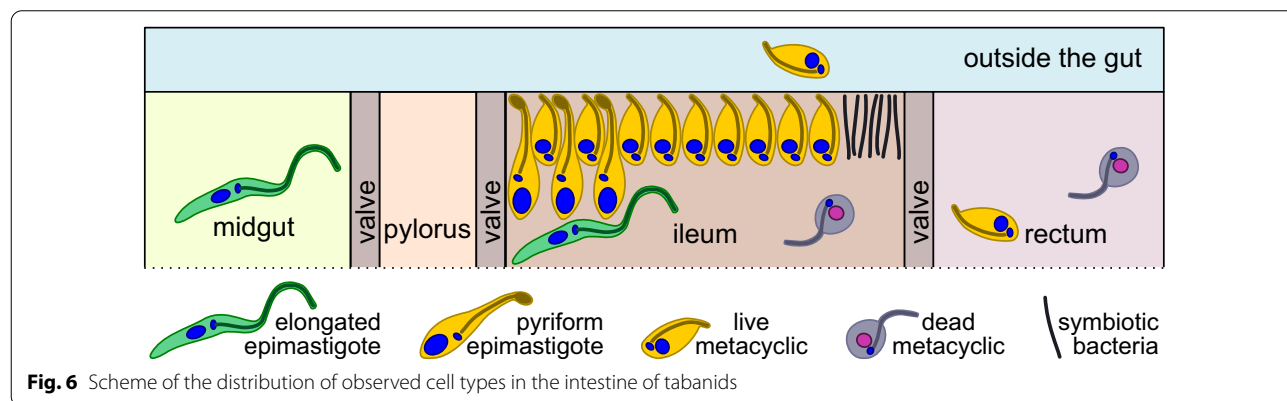
margin (Fig. 5g). In metacyclic trypomastigotes, representing the predominant morphotype, the nucleus has a subcaudal position, while the kinetoplast is placed either near the posterior margin of the latter or behind it (Fig. 5h–k).

Rare trypanosomes observed in the midgut are exclusively represented by elongated epimastigotes. In the rectum, in addition to occasional metacyclics, dead rounded cells can be observed. On Giemsa-stained smears, these cells show signs of degradation: broken

contour, “effloresced” and often vacuolized cytoplasm, etc. (Fig. 5l). Of note, such cells can also be observed in the ileum. The distribution of trypanosomes in different gut sections is summarized in Fig. 6.

Despite some variation in size and shape within each of the three cell types, we did not detect any visible differences between the two species of trypanosomes studied here. To check it statistically, we estimated standard morphometric parameters of the three cell types in six isolates belonging to both species (Additional file 1: Table S1) and subjected them to principal component analysis. Over 87% of variance could be explained by the two principal components with the

strongest contribution of cell length followed by distances between the anterior end and nucleus or kinetoplast (Additional file 3: Table S2). Confirming the previous assessment by eye, the species *Ttha* and *Tthβ* could not be reliably discriminated by any of the morphotypes (Fig. 7). However, such a difference could be observed between different isolates of a single species (Additional file 4: Fig. S2). Furthermore, in agreement with the intermediate status of the pyriform epimastigotes, they showed the largest variation and significant overlap with elongated epimastigotes and metacyclics (Fig. 7).



**Electron microscopy**

The details described in this section were observed in both Tth $\alpha$  and Tth $\beta$ ; therefore, no reference to particular isolates or species is provided. The epithelium of the

infected ileum is covered with 2–3 layers of flagellates tightly adjoining each other (Fig. 8a, d). The surface of trypanosome cells forms longitudinal ridges (Fig. 8b, c). The parasites are attached to the cuticular lining of the

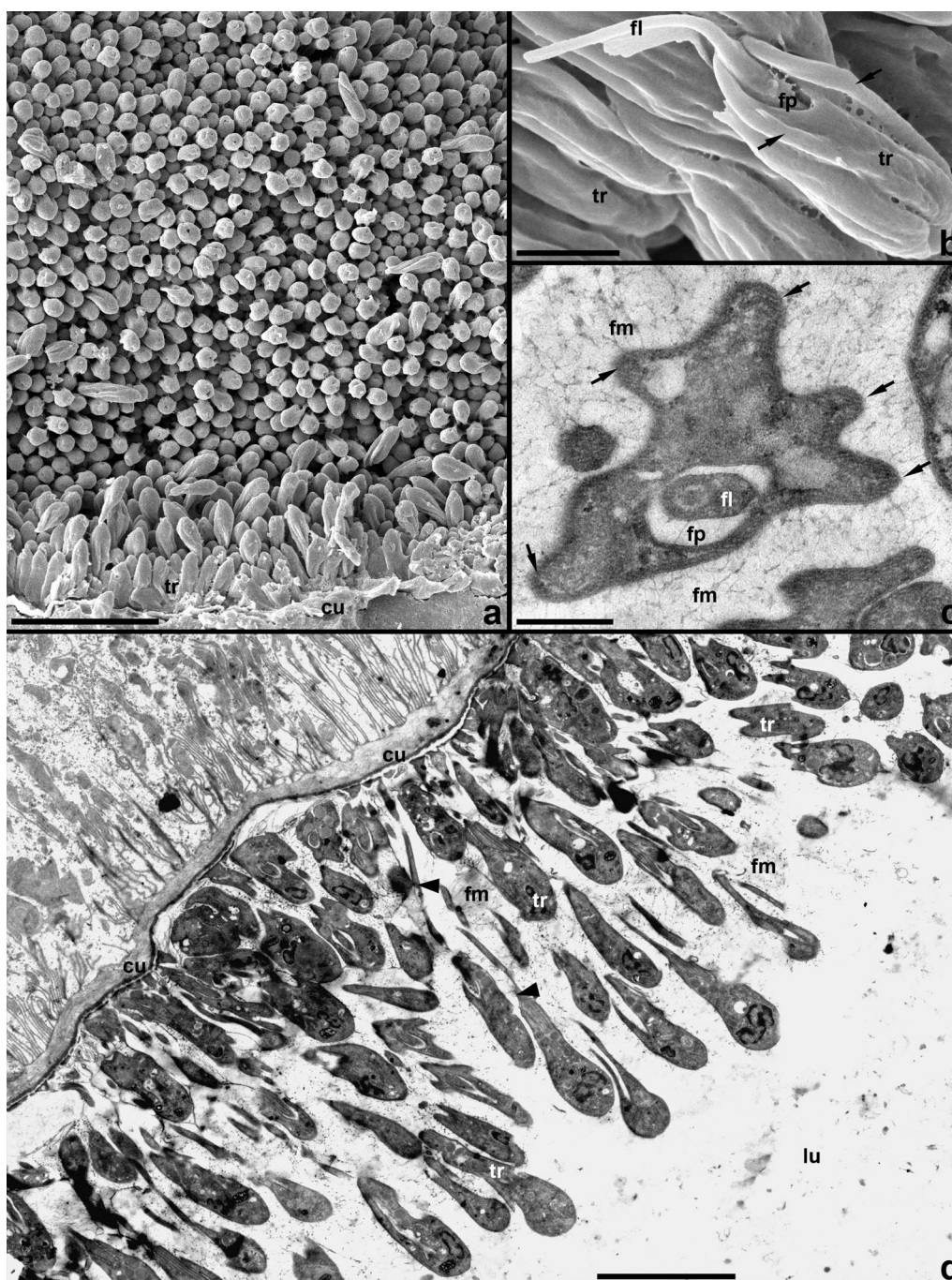


**Fig. 8** Trypanosomes occupying the cuticular lining of ileum. **a, b** SEM; **c, d** TEM. **a, d** General view. **b** Lateral view of a single cell with broken flagellum. **c** Cross section of a trypanosome cell. Arrows: longitudinal ridges; arrowheads: long flagella of cells from distal rows; *cu* cuticle, *fl* flagellum, *fm* fibrillar matrix surrounding trypanosomes, *fp* flagellar pocket, *lu* intestinal lumen, *tr* trypanosomes. Scale: **a** 10  $\mu$ m, **b** 1  $\mu$ m, **c** 0.4  $\mu$ m, **d** 4  $\mu$ m

ileum using modified flagellar tips, which form a sucker-like thickening (Figs. 8d and 9a–c). The cells of the first (proximal) row bear very short flagella, widening before the exit from the flagellar pocket (Fig. 9a, c). A zonal

hemidesmosome is formed under the plasmalemma of flagellar tips in the area of contact with the cuticle (Fig. 9a, c). Trypanosomes in distal rows use flagella of a length that allows them to attach directly to the cuticle

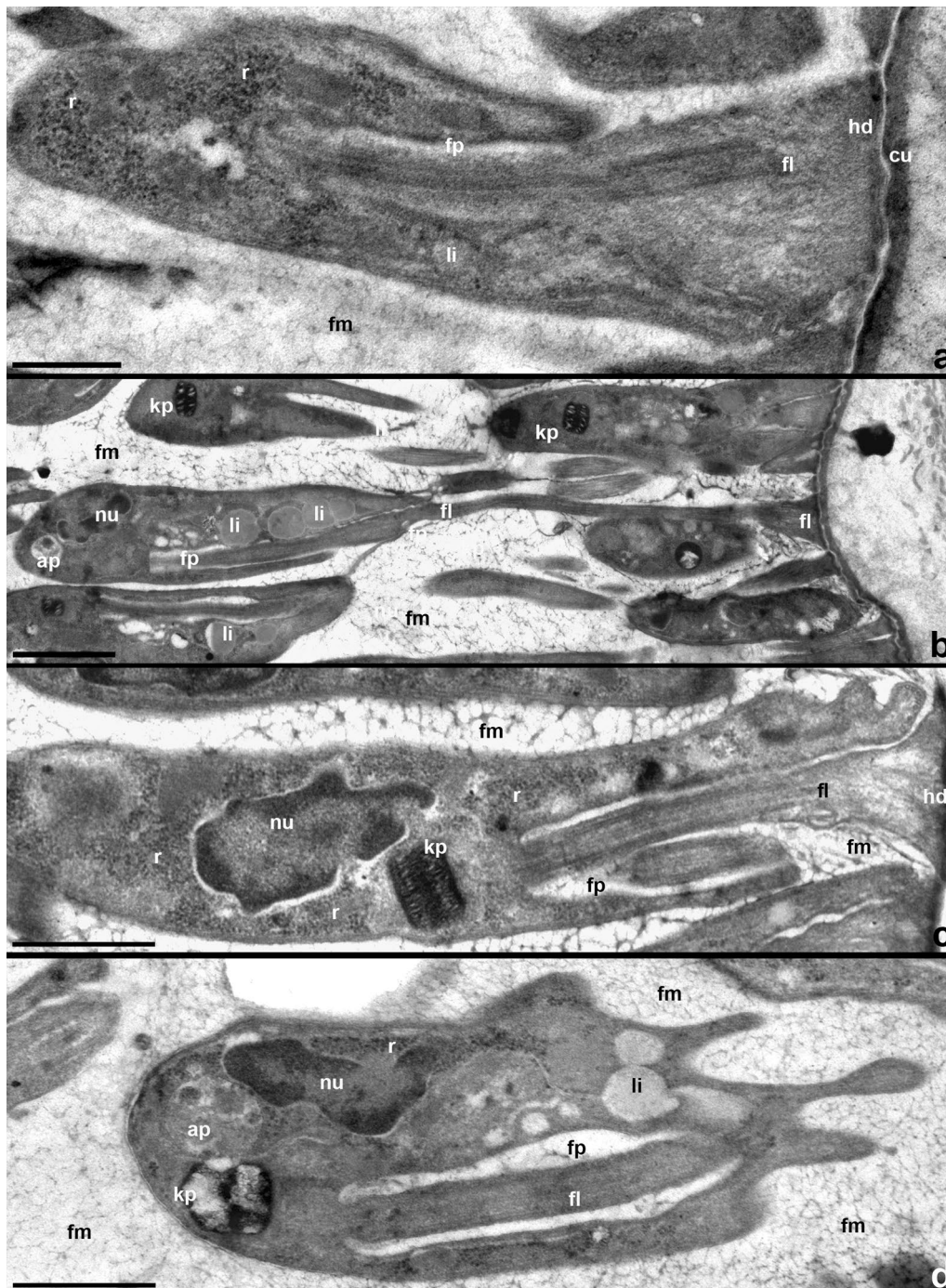


**Fig. 9** Fine structure of trypanosomes in the ileum. **a–c** Pyriiform epimastigotes. **d** Metacyclic. Cells are attached using widened tips of short (**a, b, c**) or long (**b**) flagella with a zonal hemidesmosome and surrounded by fibrillar matrix. *ap* autophagosome, *cu* cuticle, *fl* flagellum, *fm* fibrillar matrix, *fp* flagellar pocket, *hd* hemidesmosome, *kp* kinetoplast, *li* lipid droplet, *nu* nucleus, *r* ribosomes. Scale: **a** 0.6  $\mu$ m; **b, c** 2  $\mu$ m; **d** 0.8  $\mu$ m

(Figs. 8d and 9b). Therefore, despite the high density of parasites near the surface of the intestinal wall, each of them is attached individually and no specific contacts between neighboring cells are detected. However, the trypanosomes are submerged in a matrix made of fibrils with a diameter of 3–5 nm, which form a loose network associated with the plasmalemma of flagellates and fill gaps between them and the cuticular lining of the ileum (Figs. 8c, d and 9a–d). This fibrillar matrix has an integrative function, and therefore those cells that have lost connection to the intestinal wall remain in the common mass of parasites.

Trypanosomes developing in the ileum rarely display acidocalcisomes, while glycosomes could not be detected at all. Instead, their cytoplasm typically contains vacuoles with electron-light content (consistent with lipids) in the anterior half of the cell and autophagosomes in the posterior one (Fig. 9b, d). Attached epimastigotes and mature metacyclics show ultrastructural differences. The cytoplasm of the former is rich in ribosomes, which fill the space between the main cell compartments more or less evenly (Fig. 9a, c). In metacyclics, ribosomes are sparse and concentrate near the nucleus and at the cell periphery (Fig. 9d). In epimastigotes, the laterally opening flagellar pocket is short (Fig. 9a, c), while in metacyclics it extends throughout most of the cell length (Fig. 9d). These two cell types also show differences in the organization of the kinetoplast. In epimastigotes, it has a nearly rectangular profile, which measures on average  $0.56 \times 0.28 \mu\text{m}$  and demonstrates a well-discernible network of circular DNA (Fig. 9c). In metacyclics, the kinetoplast has a barrel-shaped profile measuring on average  $0.54 \times 0.43 \mu\text{m}$ . Its DNA forms condensed islands in the periphery and center, which are interconnected by looser “bridges” (Fig. 9d).

Trypanosomes can also be found on the outside of the ileum wall, between the intestinal epithelium, which is not underlain by a basal membrane, and circular muscles. In the space, enclosed between these two layers and containing tracheoles and longitudinal muscles, single cells or small groups of parasites are localized (Fig. 10a). These trypanosomes do not contact any host tissues or each other. The surface of their plasmatic membrane harbors a fibrillar glycocalyx developed to varying degrees, with thickness reaching 200 nm (Fig. 10b, d). Individual fibrils of this glycocalyx have the same diameter as those in the matrix surrounding the intestinal forms, i.e. 3–5 nm. In contrast to the cells observed in the lumen of the ileum, the overwhelming majority of extraintestinal stages display an even cell surface (Fig. 10a, b). The arrangement of the nucleus and kinetoplast in these cells indicates that they are metacyclic trypomastigotes (Fig. 10b, c). However, they differ from intestinal metacyclics by the

presence of acidocalcisomes and glycosomes, short club-shaped flagellum and the organization of kinetoplast reminiscent of that in epimastigotes (Fig. 10b, c).

## Discussion

In this work, we studied the development of the parasites belonging to two different species of the *Trypanosoma theileri* complex, which, in the absence of information on the morphology of their bloodstream forms, were provisionally designated as Tth $\alpha$  and Tth $\beta$ . Although nesting within two different clades of the complex (TthI and TthII), these two species are highly similar. Both were found in tabanid vectors and, as judged by our phylogenetic inferences, apparently represent the parasites of cervids. We were unable to discriminate these species by morphology, morphometry, ultrastructure or development in the vector. It remains unclear whether they have any differences in the vertebrate host or represent classical twin species.

Although Tth $\alpha$  and Tth $\beta$  do not show differences from each other, their development in the intestine of the vector is clearly distinct from that described for *T. melophagium* in the sheep ked *Melophagus ovinus*. The latter was shown to colonize the midgut, where elongated epimastigotes attach to the brush border of the epithelium by intertwining their flagella with microvilli and actively multiply. Then, they spread to the pylorus, ileum and rectum, attaching to the cuticle of these hindgut sections as proliferative pyriform epimastigotes and non-proliferative metacyclics [40–42]. The trypanosomes studied here do not form a stable micropopulation in the midgut (Fig. 6). Its colonization is transitory, and the reason certainly lies in the absence of attached forms within this intestinal section. This is in line with a previous study, showing that epimastigotes in the midgut of tabanids could be observed only on days 1–4 post-infection [39]. In contrast to *T. melophagium*, Tth $\alpha$  and Tth $\beta$  settle only in the ileum, ignoring the pylorus and rectum (Fig. 6). The absence of these flagellates from the latter section is especially surprising, since it is one of the preferred locations for trypanosomatids, many of which live on the surface of the rectal glands/pads or in close proximity to them [58]. This distinction may be explained by differences in the physiology of the digestive system in keds and tabanids. Regrettably, to the best of our knowledge, such studies have not been performed so far. In line with this assumption are the data on *T. theodori*, although its affiliation to the *T. theileri* complex has not been verified using molecular methods so far. The development of this trypanosome in the goat ked resembles that of *T. melophagium*, except for the presence of trypomastigotes (along with epimastigotes) in the midgut [2]. The mechanism of transmission in *T. theodori* is the same as

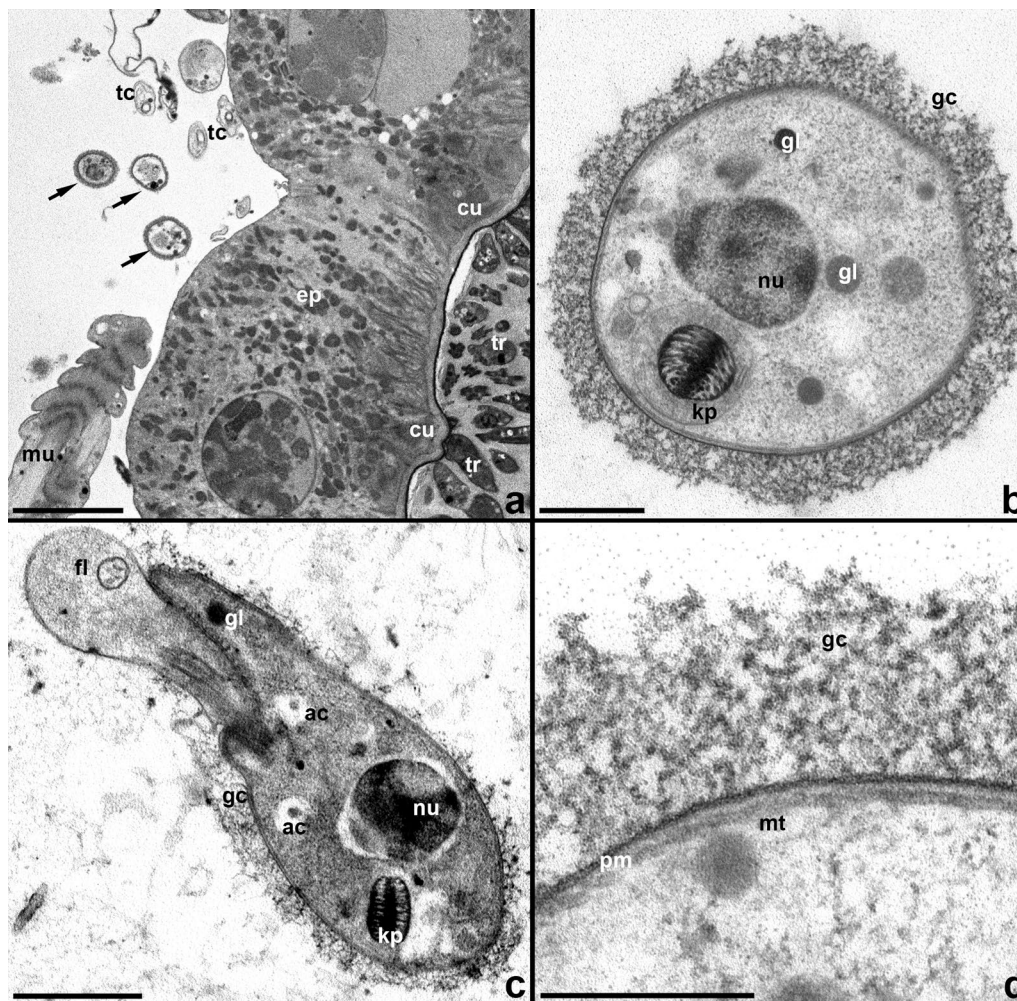


**Fig. 10** Extraintestinal trypanosome cells. **a** Trypanosomes from both sides of the intestinal wall. **b, c** Single cells, cross and longitudinal sections, respectively. **d** Cell coverings structure. *ac* acidocalcisome, *cu* cuticle, *ep* intestinal epithelium, *fl* flagellum, *gc* glycocalyx, *gl* glycosome, *kp* kinetoplast, *mt* microtubules, *mu* muscles, *nu* nucleus, *pm* plasmalemma, *tc* tracheoles, *tr* trypanosomes in the gut lumen. Arrows point to extraintestinal trypanosomes. Scale: **a** 6  $\mu$ m, **b** 0.4  $\mu$ m; **c** 1  $\mu$ m; **d** 0.2  $\mu$ m

in *T. melophagium* and very similar to that in tabanid-transmitted flagellates: contamination of oral mucosa with intestinal content released after squashing the insect either by tongue (in cows and deer [7, 34]) or teeth (in sheep and goats [2]).

One more important difference between *T. melophagium* and the trypanosomes studied here concerns the contacts between the flagella of attached forms in the hindgut, which allow them to form rosettes. The connection between cells is preserved even when such a rosette breaks away from the intestinal wall [40, 41]. These contacts were never observed in the trypanosomes from tabanids studied here. However, another mechanism that helps the attached cells to stay together, namely the formation of the fibrillar matrix surrounding the entire

mass of parasite cells attached in the hindgut, is present in all three species of trypanosomes under discussion. Previously, it has been argued that this matrix is of trypanosome origin, since it appears only in the hindgut, the cuticular lining of which prevents secretion of complex molecules [59]. Here we demonstrated that the fibrils forming the matrix are similar to those that constitute the glycocalyx layer on the surface of the cells from extraintestinal location, confirming that they are produced by the parasites.

Our detection of trypanosomes outside the ileum lumen is especially intriguing. In contrast to other trypanosomatids that traverse the intestinal wall, because it is an indispensable part of their development within the host [60–62], the exit process could not be captured here,

and we observed only its result. Furthermore, the number of parasite cells located from outside of the intestinal epithelium was always modest, further indicating that this may occur inadvertently. We hypothesize that this phenomenon is occasional and occurs after an accidental rupture of the intestinal wall, which then quickly self-heals [63]. The cells do not appear to die there, since we observed a transformation of their ultrastructure, suggesting some further development. However, they were never detected in the process of division and, therefore, may represent another kind of persistent stage, which is distinct from the intestinal metacyclics. The observed morphological changes may be related to the fact that these cells no longer need to be attached. It is not possible to judge whether the same phenomenon exists in the case of *T. melophagium*, since extraintestinal locations were not specifically assessed for that species and, due to the sparsity of the cells outside the gut, it is not possible to detect them with light microscopy except for semithin sections (Additional file 5: Fig. S3).

## Conclusions

We demonstrated that the development of flagellates of the *T. theileri* complex in vectors depends on the identity of the latter rather than on the phylogenetic position of the former. However, in general, all these trypanosomes develop similarly, which can be explained by virtually the same mode of transmission.

## Abbreviations

EDTA: Ethylenediaminetetraacetic acid; gGAPDH: Glycosomal glyceraldehyde 3-phosphate dehydrogenase; SEM: Scanning electron microscopy; SDS: Sodium dodecyl sulfate; TEM: Transmission electron microscopy.

## Supplementary Information

The online version contains supplementary material available at <https://doi.org/10.1186/s13071-022-05212-y>.

**Additional file 1: Table S1.** Summarized cell measurements.

**Additional file 2: Figure S1.** Detailed 18S rRNA gene-based tree of *T. theileri*-like trypanosomes listing accession numbers of sequences used. New sequences are marked with asterisks.

**Additional file 3: Table S2.** Loadings and proportion of variance for the two principal components.

**Additional file 4: Figure S2.** Scatterplot of the principal component analysis showing a two-dimensional space of morphometric data in three cell morphotypes individually for each isolate. PC1 and PC2: principal components 1 and 2, respectively, numbers in parentheses show the percentage of variance explained by a particular component. ee = elongated epimastigotes, pe = pyriform epimastigotes, m = metacyclics.

**Additional file 5: Figure S3.** Extraintestinal trypanosome cells on semithin sections. A: isolate 513SL, B: isolate 519SL.

## Acknowledgements

The research was completed using equipment of the "Taxon" Core Facilities Centre at the Zoological Institute Russian Academy of Sciences (St Petersburg,

Russia). The authors are grateful to Dr. Evgeny A. Genelt-Yanovskiy for his advice on principal component analysis.

## Authors' contributions

AYK and AOF designed the study. AIG, AOF, DD, MNM and VVA collected material for the study. VVA identified insects. AOF, AIG, DD and MNM performed light microscopy analyses. AIG and DD carried out statistical analyses. AIG, DD, and MNM performed electron microscopical studies. AIG, AYK and VY completed molecular analysis of trypanosome isolates. AYK inferred phylogenetic trees. AYK and AOF drafted the manuscript. AYK, AIG and AOF prepared illustrations. AYK and VY edited the final draft. All authors read and approved the final manuscript.

## Funding

This research was funded by the Russian Science Foundation Grant 21-14-00191 to AYK, AOF, MNM, AIG, DD and VVA as well as the grant from the European Regional Funds (CZ.02.1.01/16\_019/0000759) to VY. The funders had no role in study design, data collection and analysis, decision to publish or preparation of the manuscript.

## Availability of data and materials

The sequences obtained in this study were submitted to GenBank and are available under accession numbers OL855997–OL856006 (18S rRNA gene) and OL860973–OL860974 (gGAPDH gene).

## Declarations

### Ethics approval and consent to participate

Not applicable.

### Consent for publication

Not applicable.

### Competing interests

The authors declare that they have no competing interests.

### Author details

<sup>1</sup>Zoological Institute of the Russian Academy of Sciences, St. Petersburg 190121, Russia. <sup>2</sup>Life Science Research Centre, Faculty of Science, University of Ostrava, 71000 Ostrava, Czech Republic. <sup>3</sup>Martinsky Institute of Medical Parasitology, Sechenov University, Moscow 119435, Russia. <sup>4</sup>Natural-Geographical Faculty, Pskov State University, Pskov 180000, Russia.

Received: 7 December 2021 Accepted: 18 February 2022

Published online: 21 March 2022

## References

- Podlipaev SA. Catalogue of world fauna of Trypanosomatidae (Protozoa), vol. 144. Leningrad: Zoologicheskii Institut AN SSSR; 1990. (In Russian).
- Hoare CA. The trypanosomes of mammals. A zoological monograph. Oxford: Blackwell Scientific Publications; 1972.
- Bruce D, Hamerton AE, Bateman HR, Mackie FP. *Trypanosoma ingens*, n. sp. Proc R Soc Lond. 1909;81:323–4.
- Kingston N, Morton JK. *Trypanosoma cervi* sp. n. from elk (*Cervus canadensis*) in Wyoming. J Parasitol. 1975;61:17–23.
- Kingston N, Bobek B, Perzanowski K, Wita I, Maki L. Description of *Trypanosoma (Megatrypanum) stefanskii* sp. n. from roe deer (*Capreolus capreolus*) in Poland. J Helminthol Soc Wash. 1992;59:89–95.
- Garcia HA, Blanco PA, Rodrigues AC, Rodrigues CMF, Takata CSA, Campaner M, et al. Pan-American *Trypanosoma (Megatrypanum) trinaperronei* n. sp. in the white-tailed deer *Odocoileus virginianus* Zimmermann and its deer ked *Lipoptena mazamae* Rondani, 1878: morphological, developmental and phylogeographical characterisation. Parasit Vectors. 2020;13:308.
- Böse R, Friedhoff KT, Olbrich S. Transmission of *Megatrypanum* trypanosomes to *Cervus dama* by Tabanidae. J Protozool. 1987;34:110–3.
- Hoare CA. Morphological and taxonomic studies on mammalian trypanosomes. X. Revision of the systematics. J Protozool. 1964;11:200–7.

9. Doherty ML, Windle H, Voorheis HP, Larkin H, Casey M, Clery D, et al. Clinical disease associated with *Trypanosoma theileri* infection in a calf in Ireland. *Vet Rec.* 1993;132:653–6.
10. Levine ND, Watrach AM, Kantor S, Hardenbrook HJ. A case of bovine trypanosomiasis due to *Trypanosoma theileri* in Illinois. *J Parasitol.* 1956;42:553.
11. Braun U, Rogg E, Walsler M, Nehrbass D, Guscetti F, Mathis A, et al. *Trypanosoma theileri* in the cerebrospinal fluid and brain of a heifer with suppurative meningoencephalitis. *Vet Rec.* 2002;150:18–9.
12. Suganuma K, Kayano M, Kida K, Grohn YT, Miura R, Ohari Y, et al. Genetic and seasonal variations of *Trypanosoma theileri* and the association of *Trypanosoma theileri* infection with dairy cattle productivity in Northern Japan. *Parasitol Int.* 2022;86:102476.
13. Hajihassani A, Maroufi S, Esmailnejad B, Khorram H, Tavassoli M, Dalir-Naghadeh B, et al. Hemolytic anemia associated with *Trypanosoma theileri* in a cow from Kurdistan province, West of Iran. *Vet Res Forum.* 2020;11:191–3.
14. Greco A, Loria GR, Dara S, Luckins T, Sparagano O. First isolation of *Trypanosoma theileri* in Sicilian cattle. *Vet Res Commun.* 2000;24:471–5.
15. Seifi HA. Clinical trypanosomiasis due to *Trypanosoma theileri* in a cow in Iran. *Trop Anim Health Prod.* 1995;27:93–4.
16. Villa A, Gutierrez C, Gracia E, Moreno B, Chacon G, Sanz PV, et al. Presence of *Trypanosoma theileri* in Spanish cattle. *Ann N Y Acad Sci.* 2008;1149:352–4.
17. Matsumoto Y, Sato A, Hozumi M, Ohnishi H, Kabeya M, Sugawara M, et al. A case of a Japanese black cow developing trypanosomiasis together with enzootic bovine leukosis. *J Jpn Vet Med Assoc.* 2011;64:941–5.
18. Sood NK, Singla LD, Singh RS, Uppal SK. Association of *Trypanosoma theileri* with peritonitis in a pregnant cross-bred cow: a case report. *Vet Med.* 2011;56:82–4.
19. Rodrigues AC, Garcia HA, Ortiz PA, Cortez AP, Martinkovic F, Paiva F, et al. Cysteine proteases of *Trypanosoma (Megatrypanum) theileri*: cathepsin L-like gene sequences as targets for phylogenetic analysis, genotyping diagnosis. *Parasitol Int.* 2010;59:318–25.
20. Fisher AC, Schuster G, Cobb WJ, James AM, Cooper SM, PerezdeLeon AA, et al. Molecular characterization of *Trypanosoma (Megatrypanum) spp.* infecting cattle (*Bos taurus*), white-tailed deer (*Odocoileus virginianus*), and elk (*Cervus elaphus canadensis*) in the United States. *Vet Parasitol.* 2013;197:29–42.
21. Suganuma K, Kondoh D, Sivakumar T, Mizushima D, Elata ATM, Thekiso OMM, et al. Molecular characterization of a new *Trypanosoma (Megatrypanum) theileri* isolate supports the two main phylogenetic lineages of this species in Japanese cattle. *Parasitol Res.* 2019;118:1927–35.
22. Pacheco TDA, Marcili A, Costa APD, Witter R, Melo ALT, Boas RV, et al. Genetic diversity and molecular survey of *Trypanosoma (Megatrypanum) theileri* in cattle in Brazil's western Amazon region. *Rev Bras Parasitol Vet.* 2018;27:579–83.
23. Hamilton PB, Adams ER, Njiokou F, Gibson WC, Cuny G, Herder S. Phylogenetic analysis reveals the presence of the *Trypanosoma cruzi* clade in African terrestrial mammals. *Infect Genet Evol.* 2009;9:81–6.
24. Rosyadi I, Setsuda A, Eliakunda M, Takano A, Maeda K, Saito-Ito A, et al. Genetic diversity of cervid *Trypanosoma theileri* in Honshu sika deer (*Cervus nippon*) in Japan. *Parasitology.* 2021;148:1636–47.
25. Rodrigues AC, Paiva F, Campaner M, Stevens JR, Noyes HA, Teixeira MM. Phylogeny of *Trypanosoma (Megatrypanum) theileri* and related trypanosomes reveals lineages of isolates associated with artiodactyl hosts diverging on SSU and ITS ribosomal sequences. *Parasitology.* 2006;132:215–24.
26. Calzolari M, Rugna G, Clementi E, Carra E, Pinna M, Bergamini F, et al. Isolation of a trypanosome related to *Trypanosoma theileri* (Kinetoplastea: Trypanosomatidae) from *Phlebotomus perfiliewi* (Diptera: Psychodidae). *Biomed Res Int.* 2018;2018:2597074.
27. Votýpka J, Rádrová J, Skalický T, Jirků M, Jirsová D, Mihalca AD, et al. A tsetse and tabanid fly survey of African great apes habitats reveals the presence of a novel trypanosome lineage but the absence of *Trypanosoma brucei*. *Int J Parasitol.* 2015;45:741–8.
28. Schoener E, Uebleis SS, Cuk C, Nawratil M, Obwaller AG, Zechmeister T, et al. Trypanosomatid parasites in Austrian mosquitoes. *PLoS ONE.* 2018;13:e0196052.
29. Morzaría SP, Latif AA, Jongejan F, Walker AR. Transmission of a *Trypanosoma sp.* to cattle by the tick *Hyalomma anatolicum anatolicum*. *Vet Parasitol.* 1986;19:13–21.
30. Latif AA, Bakheit MA, Mohamed AE, Zwegarth E. High infection rates of the tick *Hyalomma anatolicum anatolicum* with *Trypanosoma theileri*. *Onderstepoort J Vet Res.* 2004;71:251–6.
31. Martins JR, Leite RC, Doyle RL. Trypanosomatids like *Trypanosoma theileri* in the cattle tick *Boophilus microplus*. *Rev Bras Parasitol Vet.* 2008;17:113–4.
32. Burgdorfer W, Schmidt ML, Hoogstraal H. Detection of *Trypanosoma theileri* in Ethiopian cattle ticks. *Acta Trop.* 1973;30:340–6.
33. Morel N, Thompson CS, Rossner MV, Mangold AJ, Nava S. A *Trypanosoma* species detected in *Rhipicephalus (Boophilus) microplus* ticks from Argentina. *Ticks Tick Borne Dis.* 2021;12:101573.
34. Böse R, Friedhoff KT, Olbrich S, Büscher G, Domeyer I. Transmission of *Trypanosoma theileri* to cattle by Tabanidae. *Parasitol Res.* 1987;73:421–4.
35. Hoare CA. An experimental study of the sheep-trypanosome (*T. melophagium* Flu, 1908), and its transmission by the sheep-keed (*Melophagus ovinus* L.). *Parasitology.* 1923;15:365–424.
36. Léger L. Sur un nouveau flagellé parasite des tabanides. *C R Soc Biol.* 1904;57:613–5.
37. Patton WS. The life-cycle of a species of *Crithidia* parasitic in the intestinal tracts of *Tabanus hilarius* and *Tabanus sp.?* *Arch Protistenk.* 1909;15:333–62.
38. Flu PC. Über die Flagellaten im Darm von *Melophagus ovinus*. *Arch Protistenk.* 1908;12:147–53.
39. Böse R, Heister NC. Development of *Trypanosoma (M.) theileri* in tabanids. *J Eukaryot Microbiol.* 1993;40:788–92.
40. Molyneux DH. *Trypanosoma (Megatrypanum) melophagium*: modes of attachment of parasites to mid-gut, hindgut and rectum of the sheep keed, *Melophagus ovinus*. *Acta Trop.* 1975;32:65–74.
41. Molyneux DH, Selkirk M, Lavin D. *Trypanosoma (Megatrypanum) melophagium* in the sheep keed, *Melophagus ovinus*. A scanning electron microscope (SEM) study of the parasites and the insect gut wall surfaces. *Acta Trop.* 1978;35:319–28.
42. Martinkovic F, Matanovic K, Rodrigues AC, Garcia HA, Teixeira MM. *Trypanosoma (Megatrypanum) melophagium* in the sheep keed *Melophagus ovinus* from organic farms in Croatia: phylogenetic inferences support restriction to sheep and sheep keds and close relationship with trypanosomes from other ruminant species. *J Eukaryot Microbiol.* 2012;59:134–44.
43. Ganyukova AI, Zolotarev AV, Malysheva MN, Frolov AO. First record of *Trypanosoma theileri*-like flagellates in horseflies from Northwest Russia. *Protistology.* 2018;12:223–30.
44. Maslov DA, Lukeš J, Jirků M, Simpson L. Phylogeny of trypanosomes as inferred from the small and large subunit rRNAs: implications for the evolution of parasitism in the trypanosomatid protozoa. *Mol Biochem Parasitol.* 1996;75:197–205.
45. Kostygov AY, Frolov AO. *Leptomonas jaculum* (Leger, 1902) Woodcock 1914: a leptomonas or a blastocrithidia? *Parazitologija.* 2007;41:126–36 (In Russian).
46. Hamilton PB, Stevens JR, Gaunt MW, Gidley J, Gibson WC. Trypanosomes are monophyletic: evidence from genes for glyceraldehyde phosphate dehydrogenase and small subunit ribosomal RNA. *Int J Parasitol.* 2004;34:1393–404.
47. Losev A, Grybchuk-Ieremenko A, Kostygov AY, Lukeš J, Yurchenko V. Host specificity, pathogenicity, and mixed infections of trypanoplasms from freshwater fishes. *Parasitol Res.* 2015;114:1071–8.
48. Katoh K, Standley DM. MAFFT multiple sequence alignment software version 7: improvements in performance and usability. *Mol Biol Evol.* 2013;30:772–80.
49. Minh BQ, Schmidt HA, Chernomor O, Schrempf D, Woodhams MD, von Haeseler A, et al. IQ-TREE 2: new models and efficient methods for phylogenetic inference in the genomic era. *Mol Biol Evol.* 2020;37:1530–4.
50. Kalyaanamoorthy S, Minh BQ, Wong TKF, von Haeseler A, Jermiin LS. ModelFinder: fast model selection for accurate phylogenetic estimates. *Nat Methods.* 2017;14:587–9.
51. Ronquist F, Teslenko M, van der Mark P, Ayres DL, Darling A, Höhna S, et al. MrBayes 3.2: efficient Bayesian phylogenetic inference and model choice across a large model space. *Syst Biol.* 2012;61:539–42.
52. Ganyukova AI, Frolov AO, Malysheva MN, Spodareva VV, Yurchenko V, Kostygov AY. A novel endosymbiont-containing trypanosomatid *Phytomonas borealis* sp. N. from the predatory bug *Picromerus bidens* (Heteroptera: Pentatomidae). *Folia Parasitol.* 2020;67:004.

53. Hammer Ø, Harper DAT, Ryan PD. PAST: paleontological statistics software package for education and data analysis. *Palaeontol Electron*. 2001;4:9.
54. Frolov AO, Malysheva MN, Ganyukova AI, Yurchenko V, Kostygov AY. Obligate development of *Blastocrithidia papi* (Trypanosomatidae) in the Malpighian tubules of *Pyrrhocoris apterus* (Hemiptera) and coordination of host-parasite life cycles. *PLoS ONE*. 2018;13:e0204467.
55. Richardson KC, Jarett L, Finke EH. Embedding in epoxy resins for ultrathin sectioning in electron microscopy. *Stain Technol*. 1960;35:313–23.
56. Spodareva VV, Grybchuk-Ieremenko A, Losev A, Votýpka J, Lukeš J, Yurchenko V, et al. Diversity and evolution of anuran trypanosomes: insights from the study of European species. *Parasit Vectors*. 2018;11:447.
57. Lima L, Espinosa-Alvarez O, Hamilton PB, Neves L, Takata CS, Campaner M, et al. *Trypanosoma livingstonei*: a new species from African bats supports the bat seeding hypothesis for the *Trypanosoma cruzi* clade. *Parasit Vectors*. 2013;6:221.
58. Frolov AO, Kostygov AY, Yurchenko V. Development of monoxenous trypanosomatids and phytomonads in insects. *Trends Parasitol*. 2021;37:538–51.
59. Heywood P, Molyneux DH. Ultrastructure of the fibrous matrix surrounding cells of *Trypanosoma melophagium* in the hind-gut of the sheep ked *Melophagus ovinus*. *Cytobios*. 1985;44:183–8.
60. Frolov AO, Malysheva MN, Ganyukova AI, Spodareva VV, Králová J, Yurchenko V, et al. If host is refractory, insistent parasite goes berserk: trypanosomatid *Blastocrithidia raabei* in the dock bug *Coreus marginatus*. *PLoS ONE*. 2020;15:e0227832.
61. Frolov AO, Malysheva MN, Ganyukova AI, Spodareva VV, Yurchenko V, Kostygov AY. Development of *Phytomonas lipae* sp. N. (Kinetoplastea: Trypanosomatidae) in the true bug *Coreus marginatus* (Heteroptera: Coreidae) and insights into the evolution of life cycles in the genus *Phytomonas*. *PLoS ONE*. 2019;14:e0214484.
62. Ellis DS, Evans DA, Stamford S. The penetration of the salivary glands of *Rhodnius prolixus* by *Trypanosoma rangeli*. *Z Parasitenkd*. 1980;62:63–74.
63. Lai-Fook J. The fine structure of wound repair in an insect (*Rhodnius prolixus*). *J Morphol*. 1968;124:37–78.

## Publisher's Note

Springer Nature remains neutral with regard to jurisdictional claims in published maps and institutional affiliations.

Ready to submit your research? Choose BMC and benefit from:

- fast, convenient online submission
- thorough peer review by experienced researchers in your field
- rapid publication on acceptance
- support for research data, including large and complex data types
- gold Open Access which fosters wider collaboration and increased citations
- maximum visibility for your research: over 100M website views per year

At BMC, research is always in progress.

Learn more [biomedcentral.com/submissions](https://biomedcentral.com/submissions)

